

Citation: Deli Zhang, Yongchang Yang, Rupeng Li, et al. Research on the coordinated control of the multi-point array support force of complex structural parts. *Journal of Harbin Institute of Technology (New Series)*. DOI:10.11916/j.issn.1005-9113.24054

Research on the Coordinated Control of the Multi-point Array Support Force of Complex Structural Parts

Deli Zhang^{1*}, Yongchang Yang², Rupeng Li³, Zhe Liu⁴ and Zheng Qin¹

(1. College of Mechanical and Electrical Engineering, Nanjing University of Aeronautics and Astronautics, Nanjing 210016, China;

2. College of Astronautics, Nanjing University of Aeronautics and Astronautics, Nanjing 210016, China;

3. COMAC Shanghai Aircraft Manufacturing Co., Ltd., Shanghai 201324, China;

4. Engineering Technology Center, Shenyang Aircraft Industry (Group) Co., Ltd., Shenyang 110850, China)

Abstract: Multi-point array flexible tooling based on multilateration is widely used in the processing and manufacturing of complex curved surface parts. However, during the positioning of workpieces, the force exerted on each flexible support point is not uniform, and there exists force coupling between the support units. In response to the force coupling problem in the multi-point array positioning support process, a coordinated control method for the support force of multi-point array positioning combining correlation coefficient and regression analysis was proposed in this paper. The Spearman correlation coefficient was adopted in this method to study the force coupling correlation between positioning points, and a mathematical model of force coupling was established between positioning units through regression analysis, which can quickly and accurately perform coordinated control of the multilateration support system, and effectively improve the force interference of the multi-point array positioning support scene.

Keywords: coordinated control; multipoint array support; positioning adjustment; flexible tooling; force control

CLC number: V263

Document code: A

Article ID: 1005-9113(2024)00-0000-08

0 Introduction

With the rapid development of the aviation manufacturing industry, flexible tooling characterized by automation, digitization, and modularization has been increasingly applied in the manufacture and assembly of aviation parts^[1-3]. The control technology for flexible positioning tooling has also emerged as popular research in the aviation manufacturing industry, mainly focusing on optimizing the machining deformation of workpieces during machining and developing control systems that incorporate digital measurement^[4-5]. Large amounts of research have been conducted globally on flexible positioning control to reduce the machining deformation of workpieces.

The research group of Professor Li^[6-7] introduced a floating positioning support method, which was

utilized to monitor the deformation of workpieces in real time through floating positioning support units, adjust the positioning based on the processing conditions of the parts, and release the deformation and residual stress of workpieces. In addition, the adjustment of the tool path strategy can process and eliminate most of the deformation progressively, which greatly improves the machining accuracy of the structural parts. On the basis of the floating positioning support method, Cheng^[8] used the genetic algorithm and the finite element method to optimize the positioning layout, including research on the optimization of the position as well as the number of floating positioning support units, which improved the dynamic stiffness of the positioning system, and reduced the machining deformation of parts. Gonzalo et al.^[9] proposed a new adaptive positioning support scheme for the geometric deformation caused by the clamping force and residual stress in the engine tail

Received 2024-07-01.

Sponsored by the Program of Shanghai Academic/Technology Research Leader (Grant No. 21XD1431200)

Corresponding Author: Deli Zhang, Ph.D, Associate Professor. Email: nuaazdl@126.com

bearing seat during machining, e.g., the workpiece was clamped with a floating positioning support to detect the deformation and force of the workpiece in real time. This scheme can reduce the machining deformation of the workpiece by controlling the reaction force of the clamping point on the workpiece, which significantly lowers the positioning time and the impact of the fixture on the machining accuracy of the workpiece. Möhring et al.^[10] placed the carbon fiber sensor between the impeller and the fixture and adjusted the fixture to achieve adaptive clamping for impeller machining by detecting the vibration of the thin-walled workpiece during machining via a sensor, thus accommodating the workpiece vibration during impeller milling.

In this paper, a coordinated control method for

the support force of multi-point array positioning combining correlation coefficient and regression analysis was proposed to address the coupling problem of support force that occurs in the positioning process of array flexible tooling.

1 Analysis of Coupling of Multi-point Array Support Force

The research object of this article is a set of self-designed composite material blade machining and adjustment fixtures, as shown in Fig. 1. This fixture adjusts the position and posture of the blades through multi-point support. Except for the base, the motion axes of each support point are independent and not connected to each other. They only make contact with the supported blade, without rigid connection.

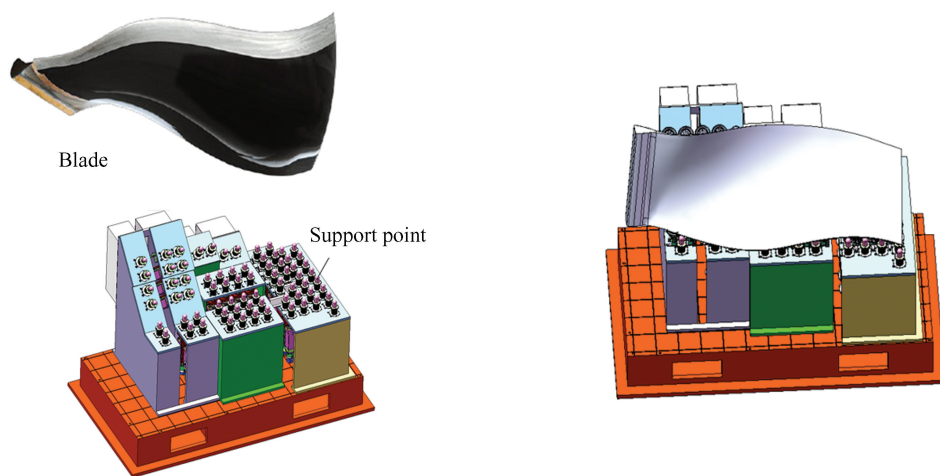


Fig.1 Multi-point array flexible positioning tooling

The multi-point array flexible tooling is based on multilateration, aiming to use accurate digital modeling to discretize the overall support surface of contact support tooling of the traditional curved surface into multiple groups of flexible support points. The flexible support array is composed of discrete points that fit the cross-section of the workpiece support. The discrete points are equivalent to a single flexible support unit, which is used to replace the traditional curved support surface, and the stroke of each flexible support unit is independently adjustable^[11].

The workpiece is mainly affected by gravity, the support force of the positioner, and the friction force in the process of multi-point array positioning^[12]. Due to the structural complexity of curved thin-walled parts^[13-14], even if a positioning support array is generated to match the curved surface of the blade

during positioning, the support force of each positioning unit on the workpiece is not uniform, resulting in deformation because of a worse distribution of clamping force on the workpiece during subsequent clamping. Therefore, the coordinated control of the positioning array should be performed to avoid excessive local support force on the workpiece during multilateration. There will be a force coupling between the positioning units in the adjustment, e.g., when a positioning unit is extended or contracted axially, the pose of the blade will be changed, so that the support force of other positioning units will accordingly change. For this reason, when the support force of a positioner is too large, its contraction cannot be controlled directly, but the force conditions of the positioners coupled with it should be evaluated to determine whether the other coupled

positioners need to be adjusted to even out the support force. The positioning module is composed of numerous positioners, so when the support force of one or some positioners exceeds the limit, it is crucial to investigate how to quickly locate the positioners coupled with them to adjust the pose accurately, while minimizing the impact on the current pose of the blade.

This paper studies the decoupling method of multi-point support forces for machining blade using the designed multi-point support fixture. The force given to each support point is calculated through this method, then distributed to each support axis. Each support axis then independently controls the force

based on the given instructions. As shown in Fig. 2, for the single force application axis, it is only a general motor + screw drive mechanism, whose stability is obvious, and this paper will not elaborate on it further. Additionally, the experimental force data curve shows that the force control did not exhibit oscillation, which verifies that the system is stable. The proposed algorithm is applied to independent motion modules of each axis that applies force, and their movements are independent of each other. However, each axis is just a universal motor+screw transmission mechanism, and its kinematics and dynamics are routine work, which will not be further described in this article.

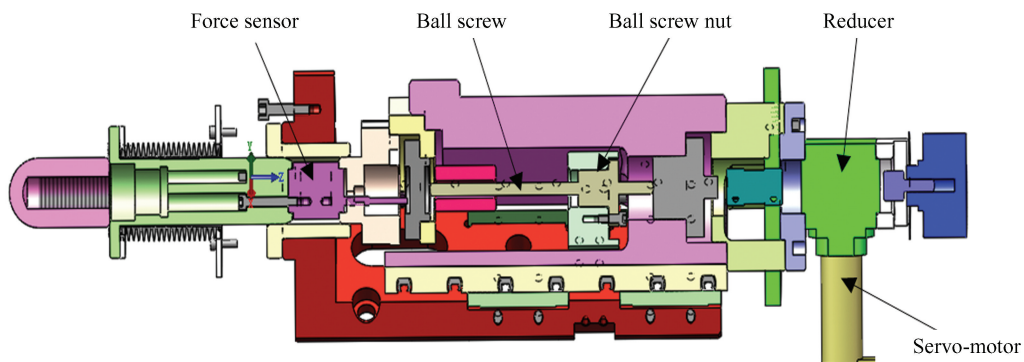


Fig. 2 Positioner structure of single point

2 Research on Coordinated Control Method for Support Force of Multi-point Array Positioning

2.1 Calculation of Spearman Rank Correlation Coefficient of Positioning Multi-point Array Support Force

In statistics, correlation analysis techniques have been applied in different fields, and the calculation of the Spearman rank correlation coefficient is a common method to measure the correlation between two variables [15-16]. The Spearman correlation coefficient was used to calculate and evaluate the correlation of support force between positioning units. As shown in Fig. 3, it is assumed that there are flexible support units a and b , when controlling a for a certain distance of axial extension motion, the force data sets of a and b are collected as $X = \{X_1, X_2, \dots, X_n\}$ and $Y = \{Y_1, Y_2, \dots, Y_n\}$, which are sorted in the ascending or descending order to obtain two sorted sets of elements $x = \{x_1, x_2, \dots, x_n\}$ and $y = \{y_1, y_2, \dots, y_n\}$. The position of each element X_i in the set

X is denoted as a_i in the set x , and that of each element Y_i in the set Y denoted as b_i in the set y to obtain the ranking sets a and b corresponding to X and Y . Each element in the sets a and b was correspondingly subtracted to obtain the ranking difference set d , where $d_i = a_i - b_i$. The Spearman correlation coefficient between X and Y can be obtained from d , as shown in Eq. (1) [17]:

$$r_s = 1 - \frac{6 \sum_{i=1}^n d_i^2}{n \cdot (n^2 - 1)} \quad (1)$$

The value range of r_s is $[-1, 1]$, and the closer the absolute value of r_s is to 1, the closer the data sample sets X and Y are to complete monotonic correlation. $r_s < 0$ means that X and Y are negatively correlated, i.e., when $r_s > 0$, X and Y are positively correlated, and when $r_s = 0$, X and Y are not correlated at all. When the support force of a positioning unit is too large, select a positioning unit that is negatively correlated with its force, that is, the Spearman correlation coefficient is less than 0, to adjust and reduce the support force of that positioning unit.

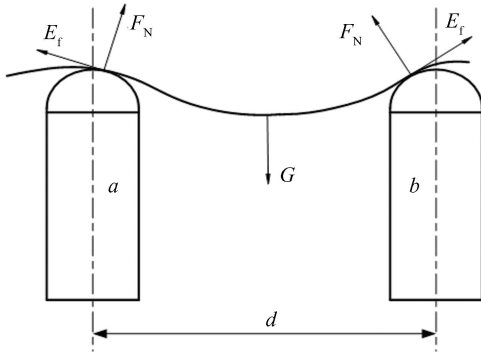


Fig. 3 Coupling of support force of multi-point array support

2.2 Force Coupling Modeling Based on Ordinary Least Squares (OLS)

There are many ways to optimize the solution, and the latest research hotspot is to use machine learning methods. However, machine learning requires a large dataset to support it, and the computation is complex. Ordinary Least Squares (OLS) method is a commonly used optimization method, which is simple to compute and easy to implement. What's more, it can meet the needs of the calculation in this paper, so OLS method is adopted in this paper. OLS is a commonly used method for solving curve fitting problems to minimize the square sum of errors and calculate the polynomial regression model with the best fitting degree to the sample data^[18]. It can be used to approximate the fit of an arbitrary nonlinearly related function model by increasing the polynomial order numbers.

It is assumed that there is a sample data set $(x_i, y_i) (i = 0, 1, \dots, m)$ whose fitting function is set as follows:

$$f(x_i) = \theta_0 + \theta_1 x_i + \theta_2 x_i^2 + \dots + \theta_n x_i^n \quad (2)$$

where n is the maximum order of the fitting function, $\theta_j (j = 0, 1, \dots, n)$ is each coefficient of the polynomial, and the square sum of errors of the fitting function can be obtained as follows:

$$S(\theta_0, \theta_1, \dots, \theta_n) = \sum_{i=0}^m [f(x_i) - y_i]^2 \quad (3)$$

Since each coefficient θ_j results in the minimum value of the square sum of errors S , the partial derivatives of S with respect to each polynomial coefficient θ_j should satisfy Eqs. (4) and (5).

$$\frac{\partial S}{\partial \theta_j} = \sum_{i=1}^m [2(\theta_0 + \theta_1 x_i + \dots + \theta_n x_i^n - y_i) x_i^j] = 0 \quad (4)$$

$$\begin{bmatrix} m & \sum_{i=1}^m x_i & \sum_{i=1}^m x_i^2 & \dots & \sum_{i=1}^m x_i^n \\ \sum_{i=1}^m x_i & \sum_{i=1}^m x_i^2 & \sum_{i=1}^m x_i^3 & \dots & \sum_{i=1}^m x_i^{n+1} \\ \sum_{i=1}^m x_i^2 & \sum_{i=1}^m x_i^3 & \sum_{i=1}^m x_i^4 & \dots & \sum_{i=1}^m x_i^{n+2} \\ \vdots & \vdots & \vdots & \ddots & \vdots \\ \sum_{i=1}^m x_i^n & \sum_{i=1}^m x_i^{n+1} & \sum_{i=1}^m x_i^{n+2} & \dots & \sum_{i=1}^m x_i^{2n} \end{bmatrix} \begin{bmatrix} \theta_0 \\ \theta_1 \\ \theta_2 \\ \vdots \\ \theta_n \end{bmatrix} =$$

$$\begin{bmatrix} \sum_{i=1}^m y_i \\ \sum_{i=1}^m (x_i y_i) \\ \sum_{i=1}^m (x_i^2 y_i) \\ \vdots \\ \sum_{i=1}^m (x_i^n y_i) \end{bmatrix} \quad (5)$$

Each coefficient θ_j of the fitting function f can be solved from Eq. (5), and the fitting calculation is completed.

In the process of fine-tuning the positioning array, there is a nonlinear relationship between the support force of a positioning unit and the displacement of its coupling positioning unit, which can be expressed as Eq. (6):

$$F_1 = f_{F_1}(x_0) \quad (6)$$

where F_1 refers to the support force of the target positioning unit to be adjusted, and x_0 represents the displacement of the coupling positioning unit of the target positioning unit. In this paper, OLS was used to establish a mathematical model of force coupling between positioning units, with the displacement of the coupling positioning unit as the input and the force of the target positioning unit as the output.

2.3 Coordinated Control Process for Support Force of Multi-point Array Positioning

Based on the characteristics of multi-point array flexible positioning support, a coordinated control method for force combining correlation coefficient and regression analysis was introduced in this paper. When the support force of a positioning unit of the positioning multi-point array exceeds the limit, the target positioning unit coupled with it can be located quickly and accurately for adaptive fine-tuning, thus

coordinating the control of support force on the workpiece. The process of the coordinated control method for support force of multi-point array positioning is as follows:

Step 1: Motion data acquisition of multi-point array positioning. In the dynamics software, the positioning process of the workpiece on the tooling was simulated as follows: Firstly, each positioning unit was controlled in turn for axial fine-tuning, with the fine-tuning distance determined by the tooling structure, and the relative stability of the workpiece could not be destroyed, while the other positioning units remained stationary during fine-tuning. After that, the displacement of the positioning unit, the support force, and the spatial motion of the workpiece centroid during fine-tuning were recorded.

Step 2: Motion data processing. Firstly, the Spearman correlation coefficient between each positioning unit and other positioning units was calculated based on the support force data recorded in Step 1. Secondly, the pose influence coefficient was calculated according to the centroid motion data of the workpiece. Finally, OLS was used to establish the mathematical model of force coupling between the support force of the positioning unit and negatively-correlated force-coupling axis displacement. The pose influence coefficient of the positioning unit on the workpiece was calculated according to Eq. (7):

$$\frac{|\Delta x| + |\Delta y| + |\Delta z|}{\Delta d} \quad (7)$$

where Δx refers to the displacement of the workpiece on the axis x (mm), Δy denotes the displacement of the workpiece on the axis y (mm), Δz represents the displacement of the workpiece on the axis z (mm), and Δd means the fine-tuning distance of the positioning unit.

Step 3: Current force information acquisition of the positioning array. The force on each positioning unit in the current positioning process was obtained through the force sensor to identify the positioning unit that needed force compliance control (hereinafter referred to as the overload axis) and the positioning unit that was close to the maximum force critical value (hereinafter referred to as the overload warning axis).

Step 4: Coordinated control of support force. First, the optimal adjustment axis was determined through three rounds of screening of the coupling axis array recorded in Step 2. The overload warning axis

was located in the coupling axis array to exclude these units in round 1. In round 2, the positioning units in the coupling axis array that were positively correlated with the overload warning axis were located to exclude these units in case new overload axes were added during adjustment. In round 3, the displacement of the positioning unit in the coupling axis array was calculated according to the mathematical model of the force coupling established in Step 2. To minimize the influences on the workpiece pose, the positioning units with the smallest product of displacements and pose influence coefficients were selected as the optimal adjustment axes before the optimal adjustment axis was controlled to move axially according to the displacement calculated by the mathematical model. After each coordinated control of force, the overload axis of the positioning array was detected. If the overload axis was not cleared, the overload axis and warning axis were updated according to the force state of the current positioning array to perform another coordinated control of force.

3 Experimental Verification of Coordinated Control of Support Force of Multi-point Array Positioning

Due to budget constraints, the tooling for blade processing was not manufactured, to verify the coordinated control method for the support force of multi-point array positioning, an array-assisted support experimental system in Fig.4 was built, which was composed of four three-axis positioners.



Fig. 4 Multi-point array support experimental system

The top of each positioner is a custom-designed ball socket mechanism, which forms an S shape with the ball head mechanism at the bottom of the workpiece, which enables the motion in the three directions of x , y , and z , and completes the spatial six-degree-of-freedom positioning and pose adjustment of

the workpiece through the motion control of the positioner. The four positioners worked together to support the workpiece at multiple points, which might generate large internal forces between each other due to the manufacturing accuracy of the workpiece model and the motion errors of the positioners, and the excessive internal forces would cause the workpiece to be subjected to large pulling forces at the ball head^[19-20], thus damaging the workpiece. A three-dimensional (3D) force sensor was installed under the ball socket of the positioner, which can monitor the contact force between the ball socket support and the ball head in real time. An absolute encoder was installed at the end of the ball screw to feed back the linear displacement of each axis in real time.

The $x, y,$ and z directions of the array-assisted support experimental system were set, and the $x, y,$ and z axes of the four positioners were numbered, as shown in Fig. 5.

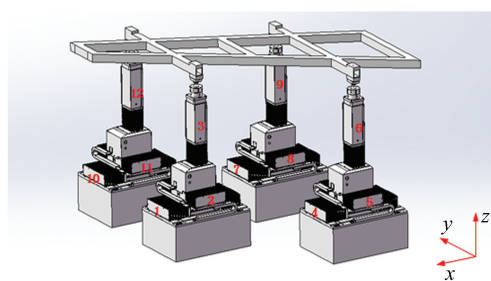


Fig. 5 Serial number of multi-point array support experimental system

The experimental steps of the coordinated control experiment for support force of multi-point array positioning are as follows:

1) The overload force and overload warning force were set according to the current force on each axis.

2) Based on the Spearman correlation coefficient and the mathematical model of force coupling, the optimal adjustment axis was screened out, and the adjustment displacement was fitted.

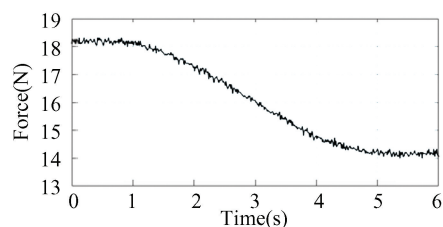
3) The optimal adjustment axis was controlled for displacement and the result was recorded.

Three groups of coordinated control experiments of forces were carried out under three different working conditions.

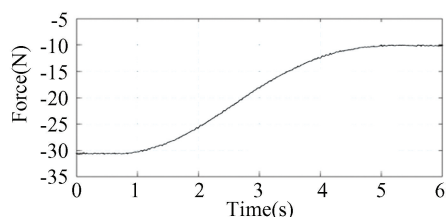
1) The overload force was set to 20 N and the overload warning force to 15 N. Fig. 6 shows the experimental results of coordinated control

experiments of forces in Group 1.

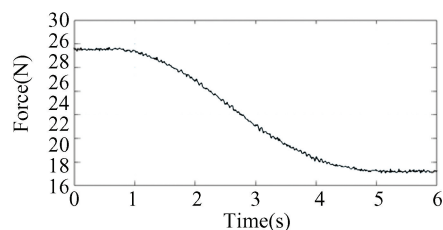
According to Fig. 6, there are overload axes No. 2 and No. 11 and overload warning axis No. 1 under the current working condition. After the coordinated control of force, the forces on overload axes No. 2 and No. 11 were reduced to below the overload critical force of 20 N, and the force on overload warning axis No. 1 was reduced synchronously.



(a) Changes in force on overload warning axis No. 1



(b) Changes in force on overload axis No. 2



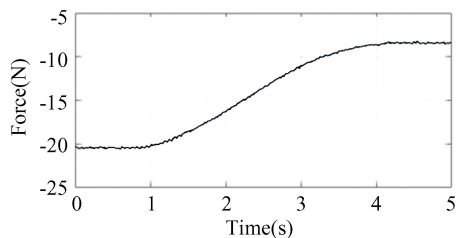
(c) Changes in force on overload axis No. 11

Fig. 6 Changes in force on the overload axis and overload warning axis (Group 1)

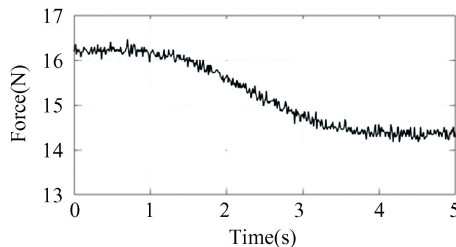
2) The overload force was set to 15 N and the overload warning force to 10 N. The experimental results of coordinated control experiments of forces in Group 2 are shown in Fig. 7.

According to Fig. 7, there are overload axes No. 2 and No. 4 and overload warning axes No. 8 and No.10 under the current working condition. After the coordinated control of force, the forces on overload axes No. 2 and No. 4 were reduced to below the overload critical force of 15 N, and the forces on overload warning axes No. 8 and No. 10 were reduced synchronously.

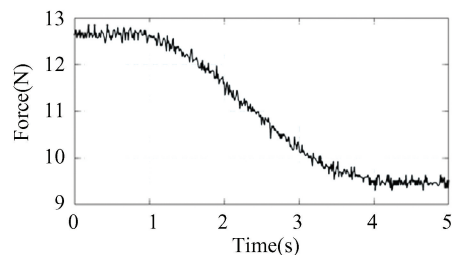
3) The overload force was set to 10 N and the overload warning force to 6 N. The experimental results of coordinated control experiments of forces in Group 3 are shown in Figure 8.



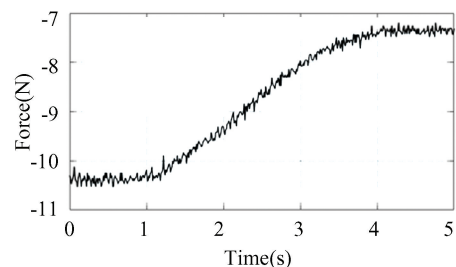
(a) Changes in force on overload axis No. 2



(b) Changes in force on overload axis No. 4



(c) Changes in force on overload warning axis No. 8

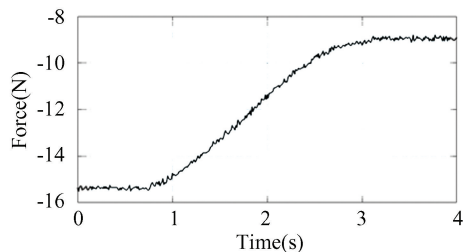


(d) Changes in force on overload warning axis No. 10

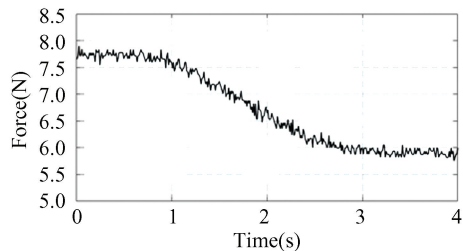
Fig. 7 Changes in forces on overload axis and overload warning axis (Group 2)

According to Fig. 8, there are overload axis No. 5 and overload warning axis No. 11 under the current working condition. After the coordinated control of force, the force on overload axis No. 5 was reduced to below the overload critical force of 10 N, and the force on overload warning axis No. 11 was reduced synchronously.

According to the above experimental results, it can be concluded that the coordinated control method for support force of multi-point array positioning can reduce the number of overloaded axes, as well as the forces of the existing overload warning axes, and improve the force interference of the multi-point array positioning support scene quickly and effectively.



(a) Changes in force on overload axis No. 5



(b) Changes in force on overload warning axis No. 11

Fig. 8 Changes in forces on overload axis and overload warning axis (Group 3)

4 Conclusions

In response to the force coupling problem in the multi-point array positioning support process, a coordinated control method for multi-point array positioning support force combining correlation coefficient and regression analysis was proposed in this paper. Firstly, the force coupling correlation between the positioning points was evaluated based on the Spearman rank correlation coefficient. Secondly, OLS was used to establish the mathematical model of force coupling between the positioning units. Finally, the optimal adjustment axis was selected by combining the Spearman correlation coefficient and regression analysis for coordinated control of force. This method can select the optimal adjustment axis quickly and accurately for coordinated control according to the force condition of the current positioning array, so as to avoid local deformation or even overall scrapping of the workpiece resulting from the excessive local support force on it during multilateration.

References

[1] Liu B F. Key technologies and development of aircraft digital flexible assembly. *Internal Combustion Engine & Parts*, 2019(22): 244-245.
 [2] Jefferson T G, Benardos P, Ratchev S. Reconfigurable assembly system design methodology: a wing assembly case study. *SAE International Journal of Materials and*

- Manufacturing, 2016, 9(1): 31–48.
- [3] Arista R, Falgarone H. Flexible best fit assembly of large aircraft components; airbus A350 XWB case study. IFIP International Conference on Product Lifecycle Management. Berlin; Springer, 2017; 152–161. DOI: 10.1007/978-3-319-72905-3_14.
- [4] Mao D C. Control on Supprot System with Flexible Clamping Function. Harbin; Harbin Institute of Technology, 2021. (in Chinese)
- [5] Fang J G, Ma Y L, LI D, et al. Integrated method of machining-measuring integration for aeroengine elliptical blade-edges. Aviation Precision Manufacturing Technology, 2016, 52(6): 1–6. DOI: 10.3969/j.issn.1003-5451.2016.06.003(in Chinese)
- [6] Li Y, Liu C, Hao X, et al. Responsive fixture design using dynamic product inspection and monitoring technologies for the precision machining of large-scale aerospace parts. CIRP Annals–Manufacturing Technology, 2015, 64(1): 173–176. DOI:10.1016/j.cirp.2015.04.025.
- [7] Wang B L, Li Y G, Hao X Z, et al. An adaptive control method of floating fixture for NC machining of complex structural parts. Aeronautical Manufacturing Technology, 2017(10): 64–69. DOI: 10.16080/j.issn1671-833x.2017.10.064.
- [8] Cheng H. Fixture Layout Optimization for Adaptive Machining of Aircraft Structural Parts. Nanjing; Nanjing University of Aeronautics and Astronautics, 2018.
- [9] Gonzalo O, Seara J M, Guruceta E, et al. A Method to minimize the workpiece deformation using a concept of intelligent fixture. Robotics and Computer – Integrated Manufacturing, 2017, 48: 209–218. DOI:10.1016/j.rcim.2017.04.005.
- [10] Möhring H C, Wiederkehr P, Lerez C, et al. Sensor integrated CFRP structures for intelligent fixtures. Procedia Technology, 2016, 26: 120–128. DOI:10.1016/j.protcy.2016.08.017.
- [11] Qu L G, Chen G T, Su C Q, et al. Design in flexible assembly tooling system of vacuum chunk for aircraft panel. Journal of Shenyang Aerospace University, 2014, 31(6): 36–41. (in Chinese)
- [12] Wu X. Design and Research of Automatic Glue Scraping Equipment for Thin-walled Wing Parts. Tianjin; Hebei University of Technology, 2020.
- [13] Yu J, Wang Y Q. Optimization of multi-point flexible fixture clamping layout for large size curved thin-walled part. Tool Engineering, 2017, 51(10): 83–87. (in Chinese)
- [14] Wu Y, Wang K F, Zheng G, et al. Review of research on flutter stability in thin wall milling with complex curved surface. Journal of Mechanical & Electrical Engineering, 2020, 37(1): 1–7.
- [15] Mohebbi A, Abdzadeh-Ziabari H, Shayesteh M G. Novel coarse timing synchronization methods in OFDM systems using fourth-order statistics. IEEE Transactions on Vehicular Technology, 2015, 64(5): 1904–1917.
- [16] Meghanathan N. Correlation coefficient analysis: centrality vs. maximal clique size for complex real-world network graphs. International Journal of Network Science, 2016, 1(1): 3–27.
- [17] Zhang W F. Statistical Analysis of Spearman’s Footrule and Gini’s Gamma. Guangzhou; Guangdong University of Technology, 2020.
- [18] Li B L. Multiple Adaptive Least Square Curve Fitting Algorithm and Applications. Jingzhou; Yangtze University, 2014.
- [19] Chen W L, Pan G W, Ding L P. Development of aircraft digital assembly technology. Aeronautical Manufacturing Technology, 2016(8): 26–30. DOI: 10.16080/j.issn1671-833x.2016.08.026
- [20] Li J C. Design of the Mobile Handling System of the Large Aireraft Parts Based on the Force Control. Shanghai; Shanghai Jiao Tong University, 2020.